

Vertical and torsional soil reactions for radially inhomogeneous soil layer

M. Hesham El Naggar†

Associate Professor and Research Director, Geotechnical Research Centre
The University of Western Ontario, London, Ontario, Canada N6A 5B9

Abstract. The response of an embedded body to dynamic loads is greatly influenced by the reactions of the soil to the motion of the body. The properties of the soil surrounding embedded bodies (e.g., piles) may be different than those of the far-field for a variety of reasons. It may be weakened or strengthened according to the method of installation of piles, or altered due to applying one of the soil strengthening technique (e.g., electrokinetic treatment of soil, El Naggar *et al.* 1998). In all these cases, the shear strength of the soils and its shear modulus vary gradually in the radial direction, resulting in a radially inhomogeneous soil layer. This paper describes an analysis to compute vertical and torsional dynamic soil reactions of a radially inhomogeneous soil layer with a circular hole. These soil reactions could then be used to model the soil resistance in the analysis of the pile vibration under dynamic loads. The soil layer is considered to have a piecewise, radial variation for the complex shear modulus. The model is developed for soil layers improved using the electrokinetic technique but can be used for other situations where the soil properties vary gradually in the radial direction (strengthened or weakened). The soil reactions (impedance functions) are evaluated over a wide range of parameters and compared with those obtained from other solutions. A parametric study was performed to examine the effect of different soil improvement parameters on vertical and torsional impedance functions of the soil. The effect of the increase in the shear modulus and the width of the improved zone is investigated.

Key words: soil reactions; soil improvement; piles; dynamic analysis.

1. Introduction

The dynamic response of piles and other embedded foundations is greatly influenced by the restraining action of the surrounding soil. Novak (1974) proposed an approximate but efficient method for the evaluation of soil impedance in which the soil is subdivided into a series of thin independent layers of infinite extent in the horizontal plane and it is assumed that waves in the soil propagate only horizontally. In this approach, soil impedances are defined as harmonic forces arising along an inner circular boundary due to a steady-state harmonic displacement of unit amplitude. Novak and Beredugo (1972), Novak (1977) and Novak and Howell (1977) computed soil impedances assuming homogeneous soil layers with uniform properties.

The soil region immediately adjacent to the foundation can experience a change in its effective properties for several reasons such as nonlinearity due to high strain levels, disturbance and remolding due to construction operations, compacting due to pile driving in cohesionless soil and

† Ph.D.

strengthening of soil adjacent to the foundation using compaction or other soil improvement techniques.

Novak and Sheta (1980) accounted approximately for the effect of the change in soil properties adjacent to the foundation. For a weakened soil, they introduced a homogeneous massless narrow annular boundary zone of reduced shear modulus and increased material damping. Other solutions were developed to account for the mass of the boundary zone. These solutions include Veletsos and Dotson (1986) and Veletsos and Dotson (1988). However, Novak and Han (1990) found that a homogeneous boundary zone with a nonzero mass yields undulating impedances due to wave reflections from the interface between the two media. In some situations, the boundary between the two media is fictitious and the undulations are artificial. Dotson and Veletsos (1990) and Han and Sabin (1995) introduced boundary zones of varying shear modulus to eliminate these undulations in the impedance functions. Dotson and Veletsos (1990) proposed including a boundary zone for which the shear modulus is considered to increase exponentially. In their model, the ratio of the change in the shear modulus and the width of the boundary zone cannot be varied arbitrarily for a specified exponent. Han and Sabin (1995) proposed a boundary zone whose shear modulus varies in a parabolic fashion. Both models are not applicable for the strengthened boundary zone.

This paper has two objectives, the first being to determine the dynamic impedances for viscoelastic layers with arbitrarily varying material properties (shear modulus and material damping) in vertical and torsional vibration modes. The results are compared with those obtained for homogeneous layers as well as for composite layers obtained using other models. The second objective is to evaluate the effect of soil strengthening on the impedance function of a soil layer and to investigate the influence of different parameters of the strengthening process to achieve the optimum treatment.

2. The composite medium

In many situations, the soil properties vary continuously within the region adjacent to the foundation. The shear modulus of the soil adjacent to a vibrating pile depends on the strain level which declines continuously with distance away from pile. The increase in the shear modulus of soil due to driving piles in cohesionless soils and the installation of tapered piles varies continuously with distance. The improvement in the clay properties using the electrokinetic treatment depends on the intensity of the electric field that varies continuously in the radial direction (El Naggar *et al.* 1998 and 1997). In all these cases, the shear modulus of the soil varies continuously in the radial direction and hence a model that represents this variation in the shear modulus of the boundary zone is implemented here.

To account for the effect of the radial inhomogeneity, it is assumed that an embedded cylindrical body of radius r_0 is surrounded by a linear viscoelastic medium composed of two concentric regions (Fig. 1(a)), an outer semi infinite undisturbed region and an inner annular boundary zone of disturbed material and width t_m . The radius of the interface of the two regions is denoted by b . The complex-valued shear modulus of the layer, $G^*(r)$, is considered to vary according to the expressions

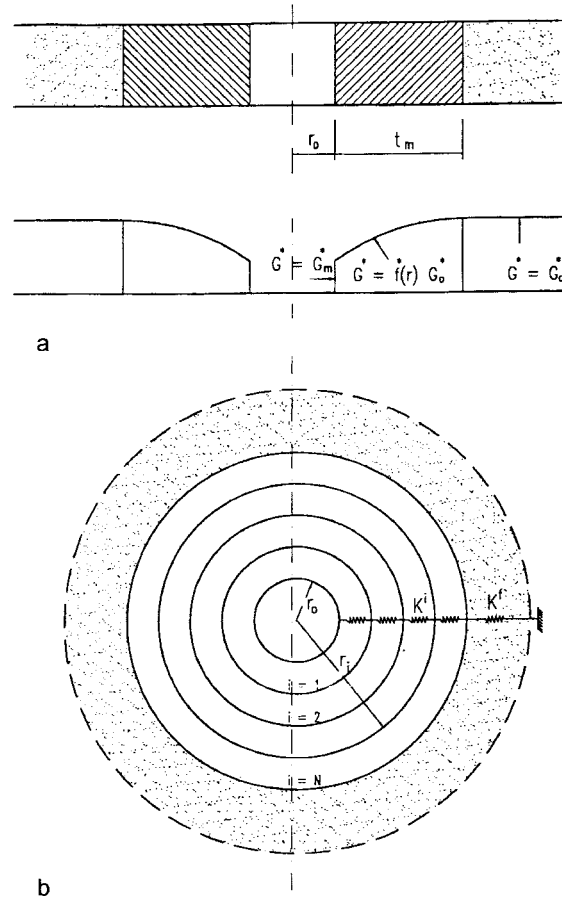


Fig. 1 Model of composite layer considered: (a) Variation of complex shear modulus with radial distance
(b) Notation for stiffness calculation of the composite layer

$$G^*(r) = \begin{cases} G_m^* & r = r_0 \\ G_0 f^*(r) & r_0 < r < b \\ G_0^* & r \geq b \end{cases} \quad (1)$$

in which

$$\begin{aligned} G_0^* &= G_0(1 + iD_0) \\ G_m^* &= G_m(1 + iD_m) \end{aligned} \quad (2)$$

where G_0 and G_m are the shear moduli of the soil layer at the outer region and the cylinder interface, respectively, and D_0 and D_m are the material damping coefficients at the same locations, respectively. The function that describes the variation of material properties within the boundary zone, $f^*(r)$, is given by the expression

$$f^*(r) = f_G(r)(1 + if_D(r)D_0) \quad (3)$$

where

$$\begin{aligned} f_G(r) &= GR - \left(\frac{r-r_0}{t_m} \right)^p (GR-1) \\ f_D(r) &= DR - \left(\frac{r-r_0}{t_m} \right)^q (DR-1) \end{aligned} \quad (4)$$

In Eq. (4), $GR = G_m/G_0$, $DR = D_m/D_0$ and p and q are positive-valued exponents. Eqs. (1) through (4) represent a continuous variation of the material properties within the boundary zone. For a strengthened boundary zone, $GR > 1$ and Eq. 4 represents a gradual decrease of the shear modulus within the boundary zone from G_m at the central hole interface to G_0 at the interface with the outer region. For a weakened boundary zone, Eq. 4 represents a gradual increase of the shear modulus within the boundary zone from G_m at the inner interface of the boundary zone to G_0 at the outer interface.

The inner region is subdivided into N concentric annular zones as shown in Fig. 1(b). Each zone is modeled as a spring whose complex constant is derived assuming a homogeneous zone with shear modulus, G^* , determined from Eqs. (2) through (4) with the pertinent radius value, r^i .

3. Soil stiffness in vertical vibration

When a homogeneous viscoelastic soil medium undergoes a vertical motion, the differential equation that governs the vertical displacement amplitudes, $w(r) = w$, is given as (Novak 1974)

$$r^2 \frac{d^2 w}{dr^2} + r \frac{dw}{dr} - s^2 r^2 w = 0 \quad (5)$$

in which

$$s = \frac{i\omega}{v_s \sqrt{1 + iD_s}} \quad (6)$$

where the shear wave velocity, $v_s = (G/\rho)^{1/2}$, ρ = mass density, D_s = material damping of soil, ω is the radial frequency and $i = \sqrt{-1}$. The solution of Eq. 5 may be written as

$$w(r) = A_w K_0(sr) + B_w I_0(sr) \quad (7)$$

in which I_0 and K_0 are the modified Bessel functions of zero order of the first and second kind, respectively, and A_w and B_w are complex-valued constants to be determined by satisfying the boundary conditions in each region.

3.1. The inner region

The inner medium is modeled as a series of springs whose constants are derived assuming homogeneous annular zones of nonzero mass, i.e., the shear modulus and material damping are considered to be constant within each annular zone and hence, Eqs. (5) through (7) hold for each zone. The stiffness of the inner medium can be obtained directly by considering the compatibility

conditions at the interface between each consecutive annular zones or by evaluating first the stiffness of each annular zone separately and joining them as with a number of springs in a series. Because of the computational convenience, the latter approach is used in this study. The same approach is used to derive the stiffness of the composite medium, i.e., the stiffness of the composite medium is evaluated from the stiffness of the inner and outer fields as with two springs in a series.

The boundary conditions for the stiffness of each zone are $w(r^{i-1})=1$ and $w(r^i)=0$, where r^{i-1} and r^i are the inner radii of zones $i-1$ and i , respectively. Applying these boundary conditions, the integration constants, A_w^i and B_w^i , are determined as

$$A_w^i = \frac{I_0(s^i r^i)}{I_0(s^i r^i)K_0(s^i r^{i-1}) - I_0(s^i r^{i-1})K_0(s^i r^i)} \quad (8)$$

$$B_w^i = -\frac{K_0(s^i r^i)}{I_0(s^i r^i)K_0(s^i r^{i-1}) - I_0(s^i r^{i-1})K_0(s^i r^i)} \quad (9)$$

where $s^i = \frac{i\omega}{v_s^i \sqrt{1+iD^i}}$, $v_s^i = \sqrt{\frac{G^i}{\rho}}$, $D^i = f_D(r)D_0$ and $G^i = f_G(r)G_0$.

The vertical stiffness of each annular zone is computed by integrating the shear stress due to harmonic displacement of a unit amplitude at the boundary interface at $r=r^{i-1}$. The resulting complex vertical stiffness is

$$K_w^i = 2\pi r^{i-1} G^{i*} (A_w^i s^i K_1(s^i r^{i-1}) - B_w^i s^i I_1(s^i r^{i-1})) \quad (10)$$

in which I_1 and K_1 are the modified Bessel functions of first order of the first and second kind, respectively. The complex vertical stiffness of the inner region is calculated as the result of a series of springs as

$$\frac{1}{K_w^I} = \sum_{i=1}^N \frac{1}{K_w^i} \quad (11)$$

3.2. The outer region

The outer region is a homogeneous medium and Eqs. (5) through (7) hold. The condition of decaying displacements with horizontal distance requires that $B_w=0$. The second boundary condition for the stiffness determination of the outer region, $w(b)=1$, is used to determine the integration constant A_w . The stiffness of the outer region is then computed by integrating the shear stress, $\tau = G_0^* \frac{dw}{dr}$, due to a harmonic displacement of a unit amplitude, $w(b)=1$, along the interface of the two regions. The resulting complex stiffness of the outer region is

$$K_w^0 = 2\pi G_0^*(s_0 b) \frac{K_1(s_0 b)}{K_0(s_0 b)} \quad (12)$$

where $s_0 = \frac{i\omega}{v_{s0} \sqrt{1+iD_0}}$.

3.3. The vertical stiffness of the composite layer

The complex stiffness of the composite medium is calculated from the stiffness of the inner and outer regions as the resultant of two springs in a series. The vertical stiffness of the composite layer is then given by

$$K_w = \frac{K_w^I K_w^0}{K_w^I + K_w^0} \quad (13)$$

For the purpose of presentation, K_w will be expressed in the form

$$K_w = \pi G_0 (S_{w1} + i a_0 S_{w2}) \quad (14)$$

in which $a_0 = \frac{\omega r_0}{v_{so}}$, $v_{so} = \sqrt{\frac{G_o}{\rho}}$, and S_{w1} and S_{w2} are real, dimensionless stiffness and damping

parameters, respectively, that depend on ω , t_m/r_0 , GR, D_0 and D_m . Figs. 2(a) and (b) show the stiffness and damping parameters, S_{w1} and S_{w2} , for a soil layer with GR=0.25; $D_m=0.1$; and $D_o=0.05$ for $t_m/r_0=1.0$ and 0.1, respectively. The number of concentric cylinders of the weak zone was varied from 1 to 20. It can be observed from Fig. 2a that increasing the number of the concentric cylinders

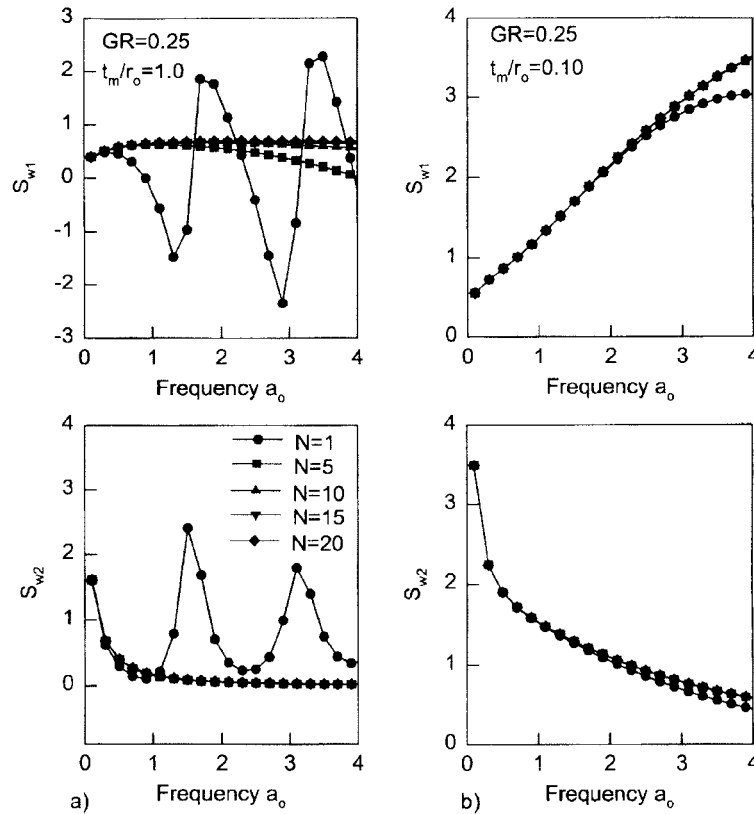


Fig. 2 Effect of number of concentric cylinders considered on computed vertical impedances (GR=0.25)
(a) $t_m/r_0=1.0$ (b) $t_m/r_0=0.1$

above 10 has virtually no effect on the solution. Also, it can be observed that the undulations are eliminated. Fig. 2b shows that 5 cylinders only are enough when $t_m/r_0=0.1$. Based on these observations, $N=10$ was assumed through the rest of this study.

3.4. Vertical impedance of composite medium with weakened boundary zone

The available solutions deal mainly with weakened boundary zones. Fig. 3 presents the comparison with some other solutions. For the sake of comparison, K_w in this figure is expressed in

the form $K_w = \pi G_m (S_{w1} + i a_m S_{w2})$ where $a_m = \frac{\omega r_0}{v_{sm}}$ and $v_{sm} = \sqrt{\frac{G_m}{\rho}}$ (because some of the other

solutions are presented in this form). The stiffness and damping parameters, S_{w1} and S_{w2} , obtained from the present analysis are presented with those obtained by Novak and Sheta (1980), N-S, Dotson and Veletsos (1990), D-V, and Han and Sabin (1995), H-S in this figure.

These solutions are for a soil layer of a unit thickness and with $t_m/r_0=1$, $GR=0.25$ and $D_m=D_0=0$. The mass density of the inner region is assumed to be equal to the mass density of the outer region in all solutions except for the N-S solution. The present solution yields results that are in good agreement with N-S solution with a slightly lower stiffness. This may be attributed to the inclusion of the mass of the inner region in the present solution while it is ignored in N-S solution. The stiffness obtained by H-S solution is influenced by the number of terms considered in the analysis (i.e., not convergent). The results presented here are calculated using 12 terms. This solution yields considerably higher stiffness and damping parameters and was found to be unstable for an improved boundary zone.

4. Soil stiffness in torsional vibration

In torsional vibration of the medium, the torsional displacement amplitude, $v(r)=v$, is governed by the differential equation

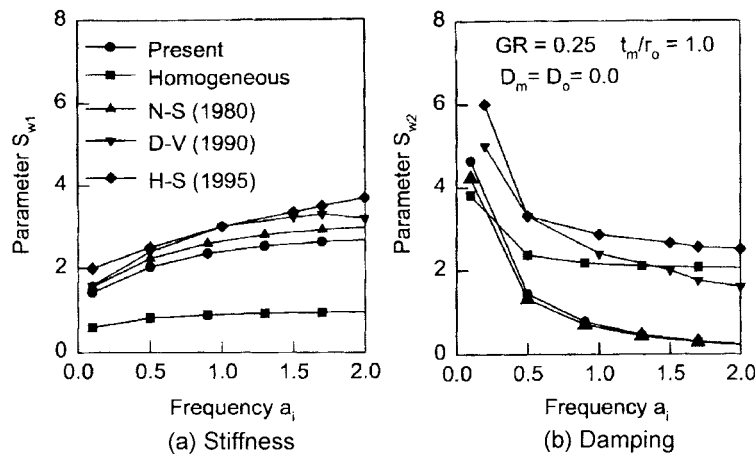


Fig. 3 Comparison of vertical impedance functions with other solutions ($t_m/r_0=1.0$, $GR=0.25$, $D_m=D_0=0.0$)

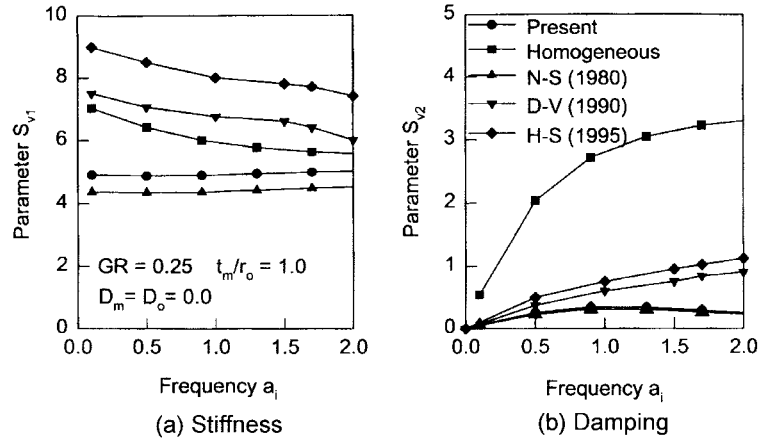


Fig. 4 Comparison of torsional impedance functions with other solutions ($t_m/r_o=1.0$, $GR=0.25$, $D_m=D_o=0.0$)

$$r^2 \frac{d^2 v}{dr^2} + r \frac{dv}{dr} - (s^2 r^2 + 1)v = 0 \quad (15)$$

The solution for Eq. 15 can be assumed in the form

$$v(r) = A_v K_1(sr) + B_v I_1(sr) \quad (16)$$

where A_v and B_v are integration constants to be determined by satisfying the boundary conditions for each region.

The same procedure applied for the vertical vibration mode is employed to develop the torsional stiffness of the composite medium. The torsional stiffness and damping parameters, S_{v1} and S_{v2} obtained from the present analysis are compared with those obtained by Novak and Sheta (1980), N-S, Dotson and Veletsos (1990), D-V, and Han and Sabin (1995), H-S in Fig. 4. These solutions are for a soil layer with $GR=0.25$, $t_m/r_o=1.0$, and $D_m=D_o=0.0$. The torsional stiffness depicted in this figure is expressed as $K_v = \pi G_m r_0^2 (S_{v1} + i a_m S_{v2})$. It may be noticed from the figure the stiffness obtained by present solution is closer to that obtained by N-S and both are less than that of the homogeneous case.

5. Effect of soil strengthening on dynamic impedances

In many situations, the soil properties adjacent to the foundation can be improved. This improvement can be due to the construction of the foundation as is the case with pile driving in cohesionless soil, installation of tapered piles and compacting the soil around massive shallow foundations. Soil improvement can also be due to the application of one of the soil improvement techniques such as jet grouting, chemical grouting, cement grouting and chemical and lime injection. However, most of these techniques are suitable for soils around and underneath inland massive foundations.

The advancement of the application of electrostatics has resulted in a novel approach for the electrical strengthening of soil by dielectrophoresis. Lo *et al.* (1994) used dielectrophoresis to strengthen natural clays. They found that the properties of the clay were improved significantly after

dielectrophoretic treatment. Experimental work done by Shang and Dunlap (1998) revealed that the electrokinetic treatment resulted in an increase of the shear strength of a marine sediment by up to 267% and an increase of the pullout resistance of steel plates, embedded in that marine sediment, by up to 88%. El Naggar *et al.* (1997 and 1998) and Abdel-Meguid *et al.* (1999) investigated the effects of this innovative technique on the response of piles installed in clay soils. They reported an increase of 41% of the axial pile capacity and 81% in the lateral pile capacity and concluded that the soil improvement is confined to the soil region adjacent to the piles. It is important to note that the strengthening of the soil in this technique is due to nonuniform cylindrical electric fields around piles. The parameters which influence the level of soil improvement are the electric field intensity, the arrangement of electrodes and their distance from each other and between the piles, and the duration of the application of the treatment. These parameters influence the increase in the shear modulus of the soil around the pile and the extent and variation of this increase.

The objective of this section is to understand the effect of the increase of the soil shear modulus and the width of the improved zone using electrokinetics on the vertical and torsional impedance of the soil layer. The exponent p is taken as 0.25 in this study. This value was found to best fit the potential distribution in the treated soil sample in an electrokinetic treatment setup (see Shang and Dunlap 1998). As the effect of this technique on the material damping is not yet known, the material damping in the improved zone is assumed to remain unchanged (i.e., $D_m=D_o=0.1$, and $q=0$) for all the results presented in this section.

Figs. 5 and 6 show the effect of the width of the improved zone (represented by t_m/r_o) on soil reactions for a soil layer with $GR=2$ in the vertical and torsional directions, respectively. It can be observed from Figs. 5a and 6a that increasing t_m/r_o results in an increase in the stiffness in the vertical and torsional directions, respectively, and the effect is more pronounced as frequency increases. However, different trends for damping may be noticed from Figs. 5b and 6b. While Fig. 5b shows that increasing t_m/r_o results in an increase in damping especially in the lower frequency range in vertical excitation, Fig. 6b shows that for torsional excitation, increasing t_m/r_o results in a decrease in the damping (except for the frequency range $a_o < 0.2$). Fig. 7 describes the effect of the increase in the shear modulus of the improved zone (represented by GR) on the vertical impedance for a soil layer with $t_m/r_o=1.0$ and different shear modulus ratios. It can be noticed from the figure

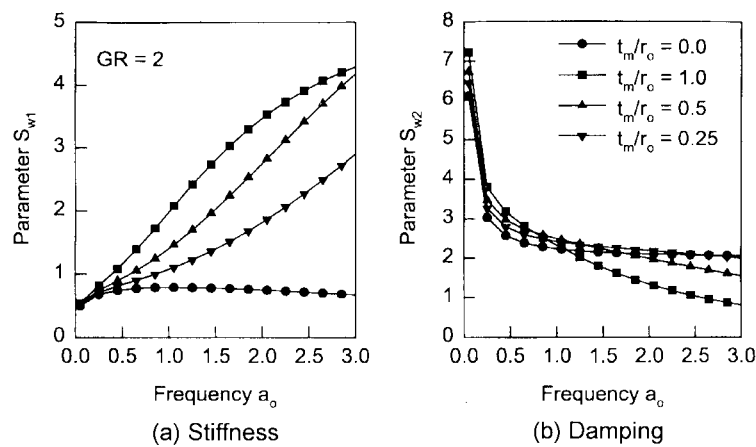


Fig. 5 Effect of width of improved zone on vertical impedance functions of soil layer ($GR=2$, $D_m=D_o=0.1$)

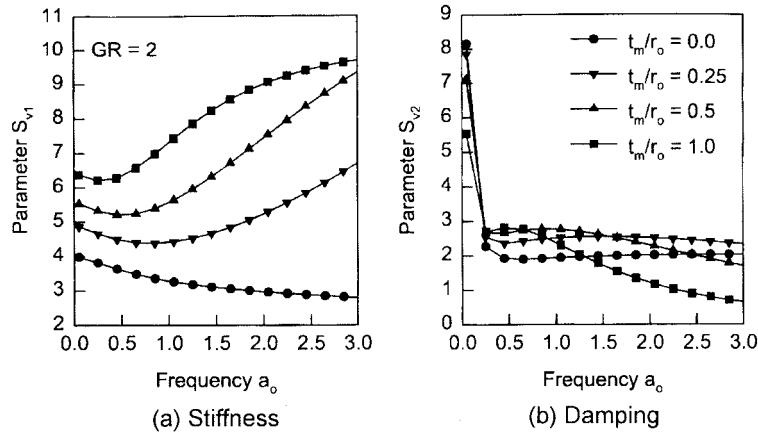


Fig. 6 Effect of width of improved zone on torsional impedance functions of soil layer ($GR=2$, $D_m=D_o=0.1$)

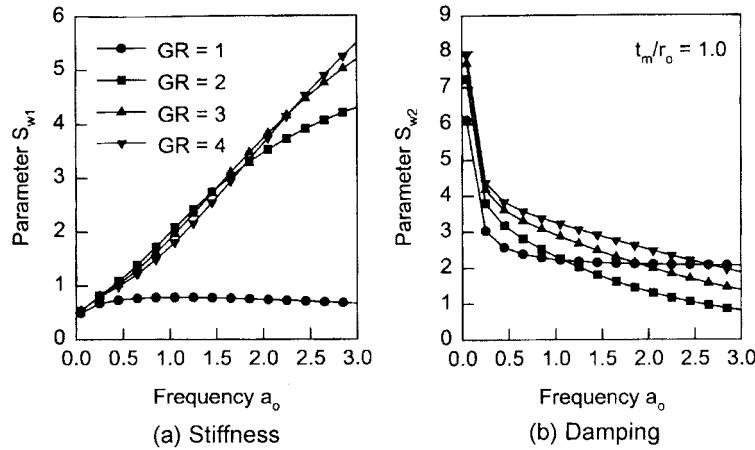


Fig. 7 Effect of shear modulus ratio of improved zone on vertical impedance functions of soil layer ($t_m/r_o=1.0$, $D_m=D_o=0.1$)

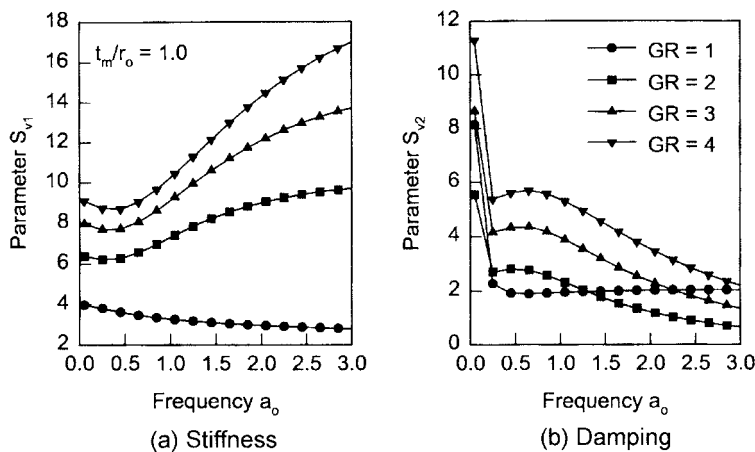


Fig. 8 Effect of shear modulus ratio of improved zone on torsional impedance functions of soil layer ($t_m/r_o=1.0$, $D_m=D_o=0.1$)

that both stiffness and damping of the layer increase with increasing GR.

Fig. 8 shows that as GR increases the torsional stiffness of the layer increases and the damping increases for $a_o < 1.5$ but decreases for higher frequencies. To illustrate the effect of a GR increase on the total torsional stiffness of the layer, $|S_v|$, Fig. 9 displays the variation of $|S_v|$ with $t_m/r_o = 1.0$ and different GR ratios. It can be noticed from the figure that the total stiffness increases as GR increases for all frequencies.

To examine the optimum combination of shear modulus ratio, GR, and improved zone ratio, t_m/r_o , Figs. 10 through 13 are presented. These combinations presumably represent approximately equal

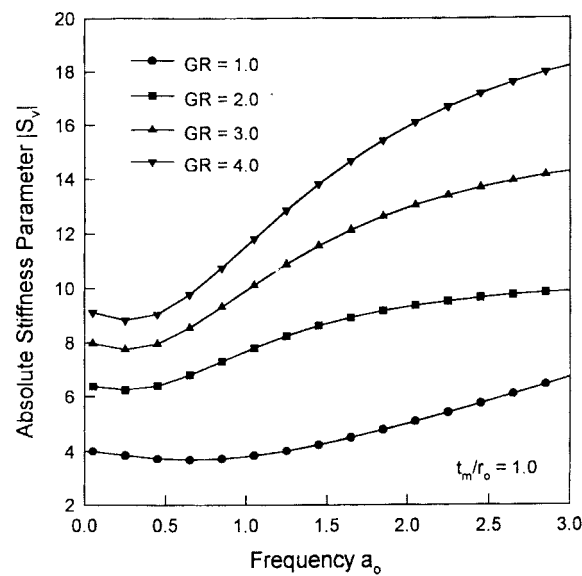


Fig. 9 Effect of shear modulus ratio of improved zone on total torsional impedance functions ($t_m/r_o = 1.0$, $D_m = D_o = 0.1$)

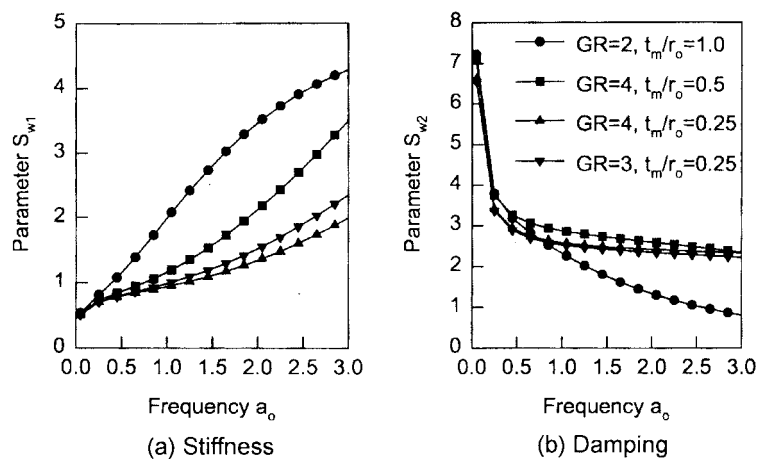


Fig. 10 Comparison of vertical impedances of soil layer with different combinations of shear modulus ratio and width of improved zone

energy consumption or improving effort. Fig. 10 shows that for vertical excitation, a soil layer with $t_m/r_o=1.0$ and $GR=2$ yields the best stiffness results but a soil layer with $t_m/r_o=0.5$ and $GR=4$ yields the best damping results. For torsional vibration, similar conclusions may be made from Fig. 11. Fig. 12 shows that in vertical excitation, a soil layer with $t_m/r_o=1.0$ and $GR=2$ would yield higher $|S_W|$ values for $a_o < 1.0$, however, as a_o exceeds 1.0 a soil layer with $t_m/r_o=0.5$ and $GR=4$ would yield higher $|S_W|$ values. The same trend is observed from Fig. 13 for the torsional vibration case.

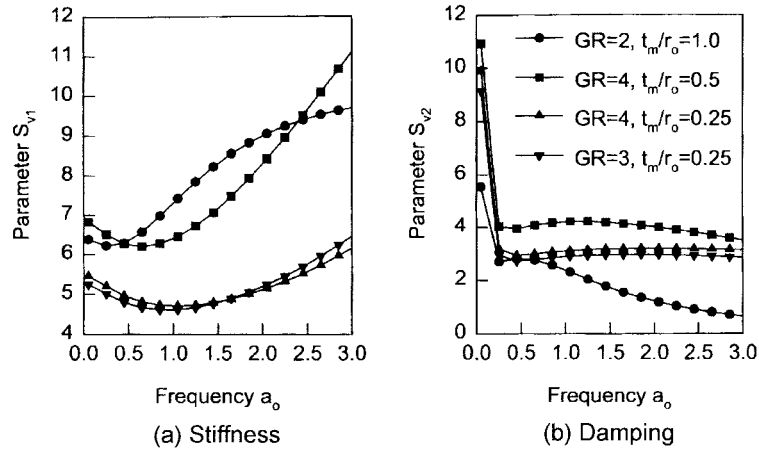


Fig. 11 Comparison of torsional impedances of soil layer with different combinations of shear modulus ratio and width of improved zone

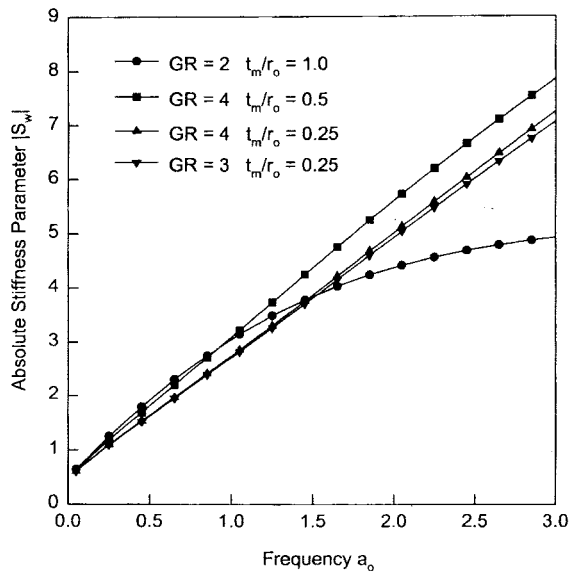


Fig. 12 Comparison of total vertical impedances of soil layer with different combinations of shear modulus ratio and width of improved zone

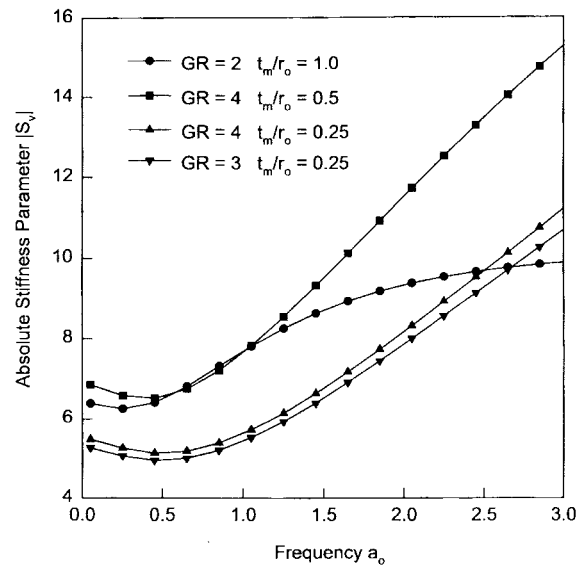


Fig. 13 Comparison of total torsional impedances of soil layer with different combinations of shear modulus ratio and width of improved zone

6. Conclusions

Vertical and torsional vibration of a radially inhomogeneous soil layer was investigated theoretically in terms of linear viscoelasticity. Solutions for vertical and torsional dynamic impedances of a radially inhomogeneous soil layer with a central cavity function were developed. The analysis proposed can model a soil layer with a radially weakened or strengthened annular zone. The soil properties within the annular zone (both shear modulus and damping ratio) may vary piecewise continuously with a smooth transition into the outer zone, so that the undulations in the impedance functions are eliminated.

The influence of improving the soil properties within the annular zone was examined. The effects of the shear modulus ratio and the width of the improved zone are studied. It was found that the optimum treatment configuration should be designed according to the frequency range of the expected excitation. For excitations with low frequency, typical of offshore environmental loads such as wind and wave, wider improved annular zones would yield higher impedance functions. For soils subjected to excitations with high frequency content, higher shear modulus ratios would result in higher soil resistance.

Acknowledgements

This study was supported by a grant from the Natural Sciences and Engineering Research Council of Canada to the author. This support is appreciated.

References

- Abdel-Meguid, M., El Naggar, M.H. and Shang, J.Q. (1999), "Axial response of piles in electrically treated clay", *Canadian Geotechnical Journal*, **36**(3), 418-429.
- Dotson, K.W. and Veletsos, A.S. (1990), "Vertical and torsional impedances for radially inhomogeneous viscoelastic soil layer", *Journal of Soil Dynamics and Earthquake Engineering*, **9**(3), 110-119.
- El Naggar, M.H., Abdel-Meguid, M.A. and Shang, J.Q. (1998), "Lateral and cyclic responses of model piles in electrically treated clay", *Journal of Ground Improvement*, **2**(4), 179-188.
- El Naggar, M.H., Shang, J.Q. and Abdel-Meguid, M. (1997), "Response of piles in electrically strengthened clay", *Proceedings, 50th Canadian Geotechnical Conference*, 738-745.
- Han, Y.C. and Sabin, G.C.W. (1995), "Impedances for radially inhomogeneous viscoelastic soil media", *Journal of Engineering Mechanics, ASCE*, **121**(9), 939-947.
- Lo, K.Y., Shang, J.Q. and Incullet, I.I. (1994), "Electrical strengthening of clays by dielectrophoresis", *Canadian Geotechnical Journal*, **31**, 192-203.
- Novak, M. (1974), "Dynamic stiffness and damping of piles", *Canadian Geotechnical Journal*, **11**(4), 574-598.
- Novak, M. (1977), "Vertical vibration of floating piles", *Journal of Engineering Mechanics, ASCE*, **103**(EM1), 153-168.
- Novak, M. and Beredugo, Y.O. (1972), "Vertical vibration of embedded footings", *Journal of Soil Mechanics and Foundations, ASCE*, **98**(SM12), 1291-1310.
- Novak, M. and Han, Y.C. (1990), "Impedances of soil layer with disturbed boundary zone", *Journal of Geotechnical Engineering, ASCE*, **116**(6), 1008-1014.
- Novak, M. and Howell, J.F. (1977), "Torsional vibration of pile foundations", *Journal of Geotechnical Engineering, ASCE*, **103**(GT4), 271-285.
- Novak, M. and Sheta, M. (1980), "Approximate approach to contact problems of piles", *Proc. of Geotech.*

- Engrg. Div., ASCE National Convention, Florida, 53-79.*
- Shang, J.Q. and Dunlap, W.A. (1998), "High voltage reinforcement of ground anchors", *J. of Geotechnical and Geoenvironmental Engineering, ASCE*, In press.
- Veletsos, A.S. and Dotson, K.W. (1986), "Impedances of soil layer with disturbed boundary zone", *Journal of Geotechnical Engineering, ASCE*, **112**(3), 363-368.
- Veletsos, A.S. and Dotson, K.W. (1988), "Vertical and torsional vibration of foundations in inhomogeneous media", *J. of Geotechnical Engineering, ASCE*, **114**(9), 1002-1021.